UV absorption by mycosporine-like amino acids in Phaeocystis antarctica Karsten induced by photosynthetically active radiation

ARTICLE *in* MARINE BIOLOGY · DECEMBER 2000

Impact Factor: 2.39 · DOI: 10.1007/s002270000424

2 AUTHORS, INCLUDING:

Tiffany Moisan
NASA
34 PUBLICATIONS **514** CITATIONS

Marine Biology (2001) 138: 217–227

T. A. Moisan · B. G. Mitchell

UV absorption by mycosporine-like amino acids in *Phaeocystis antarctica* Karsten induced by photosynthetically available radiation

Received: 31 March 1999 / Accepted: 13 July 2000

Abstract Mycosporine-like amino acids (MAAs), which occur in diverse taxonomic groups, exhibit in vivo absorption maxima between 310 nm and 360 nm and may play a photoprotective role against ultraviolet (UV) exposure. Using cultures of colonial *Phaeocystis antarctica*, we examined the relationship between MAA concentration, in vivo UV absorption, photoprotective (carotenoid) and photosynthetic pigments, and photosynthetically available radiation (PAR, 350–700 nm). UV absorption was high; chlorophyll-specific absorption, a^*_{ph}, at 330 nm ranged from 0.06 to 0.41 m^2/mg chlorophyll *a*. Values of a^*_{ph} (330) were 4–13 times greater than a^*_{ph} (676). Mycosporine-glycine, shinorine, and mycosporine-glycine valine are responsible for the strong in vivo UV absorption. The sum of all MAAs increased with irradiance when normalized to chlorophyll *a* or carbon concentrations, whereas individual MAAs varied independently from each other. Mycosporine-glycine concentrations showed no statistically significant change over the range of light intensities, whereas mycosporine-glycine and shinorine concentrations increased at higher irradiances. The relative fluorescence yield for chlorophyll *a* was low in the UV region compared to the visible region, implying that absorbed UV radiation (< 375 nm) is transferred inefficiently to chlorophyll *a* in the reaction center. Quantitative estimates of UV screening by MAAs are attributed to elevated MAA concentrations and increased diameter at high light.

Communicated by: M. H. Horn, Fullerton

T. A. Moisan (✉) · B. G. Mitchell
Marine Research Division,
Scripps Institution of Oceanography,
University of California,
La Jolla, CA 92093-0218, USA

Present address:
T. A. Moisan
NASA Goddard Space Flight Center,
Wallops Flight Facility,
Wallops Island, VA 23337-5099 USA

Fax: +1-757-824-1036
e-mail: tmoisan@osb.wff.nasa.gov

Introduction

Increases in ultraviolet-B (UV-B) radiation due to the seasonal ozone hole in Antarctica has led to concern about its impact on the regional food web and biogeochemical cycle (Smith and Cullen 1995). Stratospheric ozone depletion occurs between September and November (Lubin et al. 1989) and coincides with the initiation of phytoplankton blooms in the marginal ice edge zone (MIZ), polynyas, and coastal waters of the Antarctic Peninsula. Diatom or *Phaeocystis* blooms are common during austral spring. Together, their productivity contributes 25–67% to the total annual primary production in the Antarctic MIZ (Smith and Nelson 1986). Ozone-related UV-B inhibition of photosynthesis can occur as deep as 25 m (Smith et al. 1992) and has been observed in at least the upper 15 m (Holm-Hansen et al. 1989). The enhanced UV radiation due to ozone depletion has been estimated to reduce annual primary production by 1–12% (Smith et al. 1992; Arrigo 1994).

A considerable amount of research in the Antarctic has addressed the impact of UV radiation on phytoplankton productivity (Villafañe et al. 1995), survivability (Karentz 1991), and taxonomic composition (Helbling et al. 1992; Vernet et al. 1994). However, little is known about how phytoplankton cope with this environmental stress. Various UV-coping mechanisms by phytoplankton have been documented, including numerous DNA repair mechanisms (Mitchell and Karentz 1993), antioxidant production against radicals produced by UV photochemical reactions (Lesser et al. 1994; Dunlap and Yamamoto 1995), and vertical mixing/stratification in the ocean, which may enhance or decrease UV-induced photoinhibition (Neale et al. 1998a).

MAAs may offer a photoprotective mechanism against UV exposure by serving as a sunscreen (Lesser et al. 1996; Neale et al. 1998b). MAAs are water-soluble compounds with a cyclohexenone chromophore conjugated to a nitrogen substituent of either an amino acid or imino alcohol (Bandaranayake 1998). They exhibit absorption maxima for various MAAs ranging from 310 nm to 360 nm. MAAs are found in marine organisms such as macroalgae, echinoderms, corals, holothuroids, ascidians, zoanthids, and fish (Karentz 1994; Bandaranayake 1998). They are found intracellularly in phytoplankton such as diatoms, dinoflagellates, cyanobacteria, prymnesiophytes, and red algae (Bandaranayake 1998). MAAs may also be excreted by phytoplankton into seawater (Vernet and Whitehead 1996), and their contribution to the colored dissolved organic matter pool may play a significant role in attenuating UV radiation during bloom periods (Mitchell et al. 1989; Whitehead 1996).

The absorption band of MAAs is ideal for photoprotection since phytoplankton photosynthesis is inhibited by UV-A and UV-B wavelengths (Mitchell et al. 1989; Cullen et al. 1992; Quesada et al. 1995; Schofield et al. 1995; Herrmann et al. 1997; Neale et al. 1998b; Gomez et al. 1998). Inhibition or damage to a cell is the product of a biological weighting function (action spectrum) and the spectral intensity of light (Caldwell et al. 1986; Cullen et al. 1992; Peterson et al. 1995). Although the biological weighting function is generally elevated at shorter wavelengths, the spectral intensity declines rapidly below 330 nm. The maximum inhibition of photosynthesis in the environment is generally found in the UV-A and is due to higher fluxes of energy compared to UV-B wavelengths.

Because of its ecological importance and high UV absorption, *Phaeocystis antarctica* is an ideal species in which to characterize the relationship between in vivo UV absorption, MAA cellular content, and the factors that play a role in MAA induction. High UV absorption in *Phaeocystis* has been demonstrated in cultures and natural populations (Marchant et al. 1991; Davidson and Marchant 1994; Vernet et al. 1994; Riegger and Robinson 1997). Vernet et al. (1994) observed a 10-fold range in the ratio of a_{ph} (330):a_{ph}(675) for Antarctic peninsula populations that were dominated by *Phaeocystis pouchetii*. Life-stage is an important factor as well; single flagellated cells apparently lack significant UV absorption compared to those with a colonial growth habit (Marchant et al. 1991). The susceptibility of *Phaeocystis* to UV damage compared to other phytoplankton taxa is not clear. Several experimental approaches have suggested that *Phaeocystis* is more sensitive to UV radiation than diatoms that have significantly lower UV absorption (Davidson and Marchant 1994; Karentz and Spero 1995), whereas other studies show UV-B-induced changes in species composition favoring *Phaeocystis* over diatoms (Davidson et al. 1994). The net effect of UV-B radiation to an organism's physiological state may depend on passive sunscreening of harmful energy as well as repair mechanism from UV damage (Lesser et al. 1994).

Several studies of natural populations have suggested that MAA induction is related to irradiance (Schick et al. 1991; Karentz 1994). However, estimates of inhibition in planktonic organisms are uncertain because varying and depth-dependent rates of vertical mixing generally are not quantified, thereby complicating experimental interpretation (Neale et al. 1998b). Vernet et al. (1994) observed that UV absorption in Antarctic phytoplankton, presumably due to MAAs, was higher in surface waters and decreased at depth. The relationship between MAA synthesis and PAR intensity has been shown for dinoflagellate cultures (Carreto et al. 1990; Neale et al. 1998b). Our study examines the relationship between MAA cellular concentration, carotenoid photoprotective and photosynthetic pigments, in vivo UV absorption, and PAR for *P. antarctica*. Several studies have shown significant amounts of in vivo absorption under PAR limitation (Garcia-Pichel and Castenholz 1993; Vernet et al. 1994) and increased absorption with increased exposure to UV (Marchant et al. 1991). Because PAR and UV co-vary with each other, it is important to understand each of the components of the mechanism which contributes to the induction of MAAs. We found that changes in PAR result in large changes in UV absorption. Using model estimates for sunscreen factors combined, we estimate that MAAs in *Phaeocystis* afford significant photoprotection of from incident UV radiation by serving as passive sunscreens.

Materials and methods

Cultures of colonial *Phaeocystis antarctica* Karsten (CCMP 1374) were grown semi-continuously for 5–8 generations in f/2 medium (Guillard and Ryther 1962) at 4 °C. Cultures were diluted with fresh medium as necessary to ensure that they were nutrient-replete and "optically thin" to minimize light attenuation due to phytoplankton. Cultures were also bubbled with cold (4 °C) sterile air and grown under continuous blue light at seven intensities ranging from 14 to 542 μmol quanta m^{-2} s^{-1}. The culture system is described in Moisan and Mitchell (1999). Light from a tungsten-halogen source was transmitted through a blue theater gel. Intensity of PAR was determined with a Biospherical Instruments QSL-100 PAR scalar irradiance meter inside a culture vessel filled with distilled water. The relative spectral irradiance was estimated at the position of the incubation bottles with a Biospherical Instruments MER2040 at 13 wavelengths.

High performance liquid chromatography of MAAs

MAA concentrations were determined for five of the seven treatments. Samples ($n = 2$) were collected on Whatman GF/F filters and stored in liquid nitrogen for several months, subsequently ground in 100% methanol, extracted for 24 h and analyzed immediately thereafter. MAA samples were run in triplicate and separated by reverse-phase isocratic high performance liquid chromatography (HPLC) on a Brownlee RP-8 column (Dunlap et al. 1986). The aqueous mobile phase was 0.1% acetic acid and 80:20 methanol:water. The column was re-equilibrated for 10 min between samples with 80:20 methanol:water. MAA peaks were

detected by absorption at 315 nm and 340 nm and the elution rate was 0.8 ml min^{-1}. Individual MAAs were identified from relative retention times of standards and a Perkin Elmer LC-235 Diode array detector. Our HPLC was calibrated using a secondary MAA calibration based on a known set of standards in collaboration with Michael P. Lesser (University of New Hampshire, USA) and Kathy Walsh (University of Quebec, Canada).

Cellular in vivo absorption

In vivo whole-cell absorption properties were determined on samples concentrated ~12-fold by centrifugation. Microscopic analyses demonstrated that the colonies maintain their morphological integrity after centrifugation and subsequent re-suspension. Quadruplicate samples in 1-cm quartz cuvettes were analyzed at 1-nm intervals using an integrating sphere attached to a dual-beam Perkin Elmer Lambda 6 UV/Vis spectrophotometer. Samples were kept at low optical densities so that multiple scattering was negligible (Bricaud et al. 1983). Fresh f/2 medium was used as a reference and a blank. The value at 750 nm was subtracted from the full spectrum to partially correct for scattering error (Moisan and Mitchell 1999). Since cell diameters were 3–5 μm, setting 750 nm to zero should compensate for most scattering error since its spectral dependence from 300 to 700 nm is small (Bricaud et al. 1983; Mobley and Stramski 1997). The cellular in vivo absorption $\left[a^*_{\mathrm{ph}}(\lambda)\right]$ was calculated by dividing a_{ph} (m^{-1}) by fluorometric chlorophyll *a* concentration (mg chl *a* m^{-3}).

Pigments, diameter, and cell concentration

Chlorophyll *a* concentration ($n = 3$) was estimated fluorometrically (Holm-Hansen et al. 1965) and by HPLC ($n = 2$, Wright et al. 1991). The HPLC data include photosynthetic and accessory pigments soluble in 100% acetone extracts. Individual cell size ($n = 25$) was determined at a magnification of 1000× on samples preserved with a final concentration of 2% glutaraldehyde. Cell concentrations were estimated in Palmer-Maloney chambers at a magnification of 400×.

Estimation of photosynthetically active absorption

Fluorescence excitation spectra ($n = 3$), $F_{\mathrm{DCMU}}(\lambda)$, were obtained at ambient growth temperatures, after the addition of 200 μl of a 3-μM stock solution of 3-(3,4-dichlorophenyl)-1,1 dimethyl urea (DCMU) to ~5 ml of culture in the sample cuvette. Spectra were determined with a Spex Fluoromax spectrofluorometer at 1-nm increments with the emission monochromator set at 730 nm (Neori et al. 1988; Sakshaug et al. 1991; Sosik and Mitchell 1995; Moisan and Mitchell 1999). A Schott glass LP720 filter was used on the emission side to minimize stray excitation light. Spectra were run in sample-to-reference mode and further corrected for quantum flux of the excitation beam using the quantum counter 2,7-bis-(diethylamino) phenazoxonium perchlorate (Kopf and Heinze 1984). To estimate the photosynthetically active absorption $\left[a_{\mathrm{ps}}(\lambda)\right]$, quantum-corrected spectra, $F_{\mathrm{DCMU}}(\lambda)$, were scaled at the red peak (676) of the fluorescence excitation spectra to the corresponding peak of the whole cell in vivo chlorophyll-specific absorption spectrum,

$$a^*_{\mathrm{ps}}(\lambda,\ \mathrm{m^2(mg\,chl}\,a)^{-1}) = \frac{F_{\mathrm{DCMU}}(\lambda)a^*_{\mathrm{ph}}(676)}{F_{\mathrm{DCMU}}(676)} \quad . \tag{1}$$

Relative fluorescence yield

Absolute fluorescence is defined as,

$$F_0(\lambda) = G(\lambda)E_0(\lambda)a_{\mathrm{ph}}(\lambda)\phi f_0(\lambda) \ , \tag{2}$$

where $G(\lambda)$ is the geometric correction for the instrument, $E_0(\lambda)$ is the spectral irradiance of the excitation source, $a_{\mathrm{ph}}(\lambda)$ is the absorption by phytoplankton, and $\phi_{\mathrm{fo}}(\lambda)$ is the true quantum yield for fluorescence. Since $a^*_{\mathrm{ps}}(\lambda)$ is simply the spectral fluorescence scaled to the red absorption peak, the ratio of photosynthetic to total phytoplankton absorption is a relative fluorescence yield,

$$\phi_f(\lambda) = \frac{a_{\mathrm{ps}}(\lambda)}{a_{\mathrm{ph}}(\lambda)} \ , \tag{3}$$

representing the probability that an absorbed photon can contribute to chlorophyll *a* fluorescence. For brevity, we define ϕ_{fMAA} to be the integral of this ratio over the 300-nm to 350-nm absorption band of MAAs for our cultures.

Sunscreen factor calculation

Sunscreen factors (S) for MAA absorption were calculated with the analytical model of Garcia-Pichel (1994). The magnitude of S is an estimate of the total absorbed flux (J_{tot}) relative to a theoretical minimum absorbed flux (J_0) for absorption not attributed to the screening compound(s) of interest. The S factor is mathematically described as,

$$S = \frac{J_{\mathrm{tot}}(330) - J_0(330)}{1 - J_0(330)} \ , \tag{4}$$

where $J_{\mathrm{tot}}(330)$ is the efficiency factor for self-shading of the whole cell at 330 nm and $J_0(330)$ is the minimal efficiency factor for self shading at 330 nm, and is defined as,

$$J_{\mathrm{tot}}(330) \text{ or } J_0(330) = 1 - \frac{1}{a_{\mathrm{ph}}(330)r} - \frac{\mathrm{e}^{-2a_{\mathrm{ph}}(330)r} - 1}{2(a_{\mathrm{ph}}(330)r)^2} \ , \tag{5}$$

where $a_{\mathrm{ph}}(330)$ is the absorption (m^{-1}) at 330 nm and r is single cell radius (m). Symbols are defined in Table 1. $J_{\mathrm{tot}}(330)$ values were calculated using Eq. 5 by introducing $a_{\mathrm{ph}}(330)$ and r values from each of the seven light treatments. Values of $J_0(330)$ were estimated by two methods. The first method consisted of determining the y-intercept value from a linear regression of each of $a_{\mathrm{ph}}(330)$ and cell radius with respect to light intensity. In the second method, we used measured cell-radius values for each culture and substituted our estimate of photosynthetically active absorption, $a_{\mathrm{ps}}(330)$ for $a_{\mathrm{ph}}(\lambda)$ to calculate J_0 for each light treatment.

Table 1 Symbols used in the text

λ	Wavelength (nm)
$E_0(\lambda)$	Spectral quantum scalar irradiance (μmol quanta m^{-2} s^{-1} nm^{-1})
PAR	Photosynthetically available radiation defined as $\int_{350nm}^{700nm} E_0(\lambda)d\lambda$ (μmol quanta m^{-2} s^{-1})
$a_{\mathrm{ph}}(\lambda)$	Absorption by phytoplankton (m^{-1})
$a^*_{\mathrm{cm}}(\lambda)$	Chl-specific absorption of cellular material (m^2 mg chl a^{-1})
$a_{\mathrm{cm}}(\lambda)$	Absorption of cellular material (m^{-1})
$a^*_{\mathrm{ph}}(\lambda)$	Chl-specific absorption of phytoplankton (m^2 mg chl a^{-1})
$a^*_{\mathrm{ps}}(\lambda)$	Chl-specific absorption of photosynthetic pigments (m^2 mg chl a^{-1})
Q_{a}	Absorption efficiency (dimensionless)
r	Radius of single cell within colony (m)
J_0 (330)	Minimal efficiency factor for self-shading of a whole cell at 330 nm (dimensionless)
J_{tot} (330)	Efficiency factor for self-shading of a whole cell at 330 nm (dimensionless)
S	Sunscreen factor (dimensionless)
$F_{\mathrm{DCMU}}(\lambda)$	In vivo DCMU-enhanced fluorescence (relative units)
ϕ_{f}	Relative quantum yield for fluorescence (dimensionless)
ϕ_{fMAA}	Integrated relative fluorescence yield over the absorption band of MAAs

Absorption efficiency (Q_a) and sample preparation of a_{cm}

The absorption efficiency for single cells (Morel and Bricaud 1981) was calculated for two treatments with absorption values of unpackaged cellular material, a_{cm}, which were prepared with a French press (Johnsen et al. 1994) at pressures of 1.37×10^8 Pa and the diameter of single cells. Spectra of a_{cm} were determined in an integrating sphere attachment for a Perkin Elmer Lambda 6 dual-beam spectrophotometer. Values of a^*_{cm} (λ) were calculated by dividing a_{cm} (λ) by the fluorometric chlorophyll *a* estimate.

Results

UV absorption in relation to PAR

For our illumination system based on tungsten-halogen sources, the UV-A radiation represents a small fraction of the total irradiance. We did not estimate the irradiance below 340 nm with our spectroradiometer; values between 340 and 350 nm were approximately 0.08% of the total radiation flux (Fig. 1A). UV absorption peaked at 330 nm for the two lowest light treatments and shifted to 336 nm when irradiances were greater than 259 µmol quanta m^{-2} s^{-1} (Fig. 1B). Values of a^*_{ph} (330) ranged from 0.06 m^2 mg chl a^{-1} to 0.41 m^2 mg chl a^{-1} and increased with increasing irradiance (Fig. 1B). The ratio of a_{ph} (330) to a_{ph} (676) ranged from 4 to 13 (Fig. 1C) and the ratio of a_{ph} (330) to a_{ph} (440) ranged from 1.5 to 3.7 (Fig. 1C).

MAAs, photosynthetic and photoprotective pigmentation

HPLC confirmed that the MAAs, mycosporine-glycine, shinorine, and mycosporine-glycine valine were responsible for the UV absorption (Fig. 2A, B). The total MAA concentration normalized to chlorophyll *a* increased with light intensity, ranging from 0.74 to 2.61 nmol MAA (µg chlorophyll *a*)$^{-1}$ (Fig. 3A). Similarly, total MAA per µg carbon increased with irradiance (Fig. 3B). Individual MAAs showed different trends from that of the total MAA pool. Concentrations of mycosporine-glycine valine and shinorine increased at high light while mycosporine-glycine concentrations showed no change with light.

Table 2 summarizes HPLC data for photosynthetic and photoprotective pigments. Non-MAA photoprotective pigments normalized to chlorophyll *a* (Table 2) or on a cellular basis (Moisan and Mitchell 1999) increased at high PAR. The pool of [diadinoxanthin (DD) + diatoxanthin (DT)]:chlorophyll *a* was especially high at 542 µmol quanta m^{-2} s^{-1}. Moisan and Mitchell (1999) reported a decrease in growth rate inhibition at this intensity compared to the maximal growth rate at 259 µmol quanta m^{-2} s^{-1}, which is most likely to due to photoinhibition. This (DD + DT) pool has shown active xanthophyll cycle activity (Moisan et al. 1998). The β-carotene:chlorophyll *a* ratio increased with PAR and was highest at 542 µmol quanta m^{-2} s^{-1}. In contrast, the chlorophyll *a*-normalized photosynthetic pigments chlorophyll (c_1 + c_2 + c_3) and 19′hexanoyloxyfucoxanthin decreased at high light. The fucoxanthin:chlorophyll *a* ratio remained fairly constant over the light gradient.

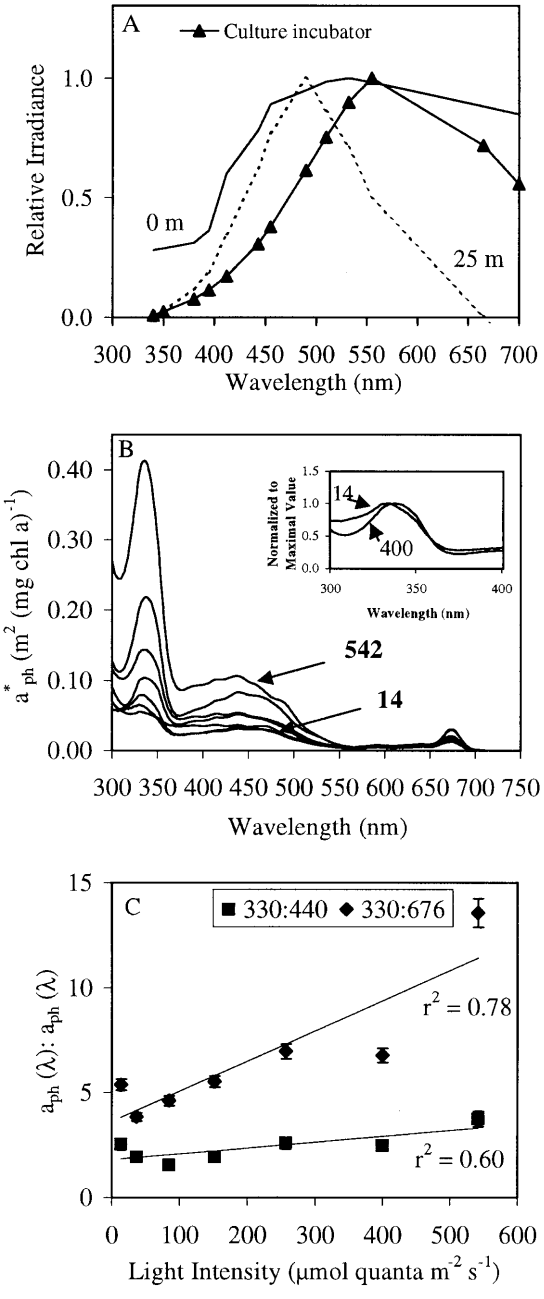

Fig. 1 **A** Relative spectral quantum irradiance used in the culture incubator compared to California coastal waters at 0 and 25-m depth. Spectra are normalized to 1.0 at their respective peaks. Symbols represent discrete points where irradiance was estimated. **B** In vivo chl-specific absorption for *Phaeocystis antarctica* grown between 14 and 542 µmol quanta m^{-2} s^{-1} at 4 °C under nutrient-replete conditions. *Inset* shows UV peaks normalized to their respective maximum for cultures grown at 14 and 400 µmol quanta m^{-2} s^{-1}. **C** The dependence of a_{ph}(330):a_{ph}(440) and a_{ph}(330):a_{ph}(676) ratios on light intensity. Linear regression is significantly different from 0 (ANOVA, $P > 0.05$)

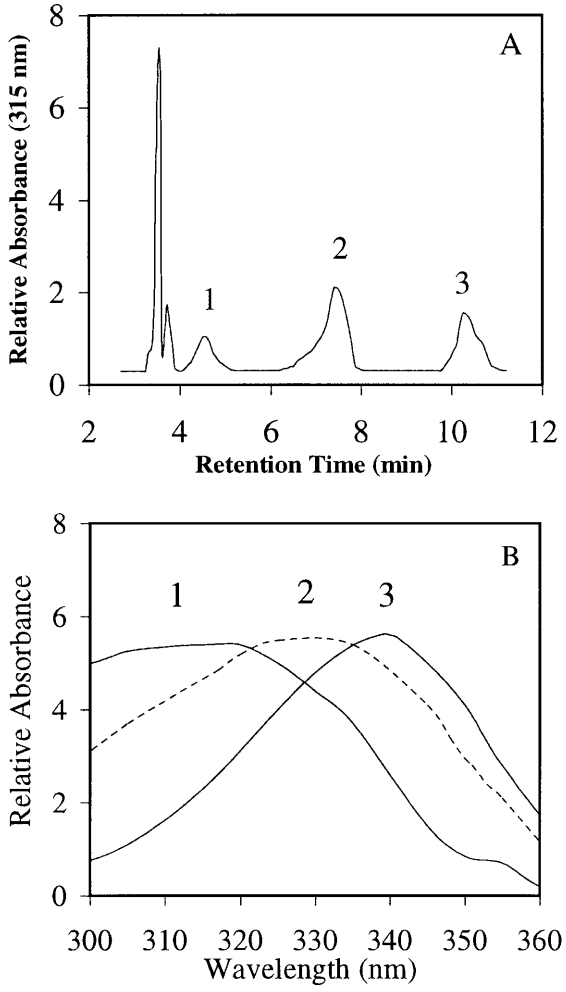

Fig. 2 **A** Example of an HPLC chromatogram showing three MAA peaks. **B** Diode-array spectra of the corresponding peaks shown in **A**. Diode-array spectra of eluted MAAs from HPLC (see Materials and methods). The peaks are: *1* mycosporine-glycine, *2* shinorine, and *3* mycosporine-glycine valine

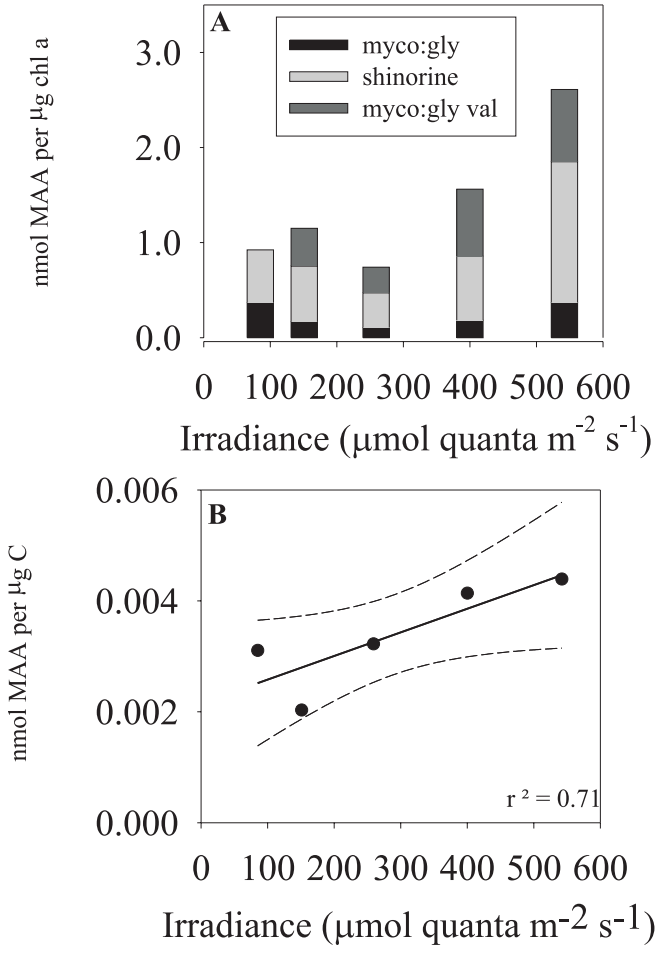

Fig. 3 A, B Light-dependence of MAA concentrations. **A** Individual MAAs per µg chlorophyll *a*. **B** Total MAAs per µg carbon. 95% confidence limits of trendline are shown in **B**. Linear regression is significantly different from 0 (ANOVA, $P > 0.05$)

Chlorophyll *a* fluorescence excitation spectra

Fluorescence excitation spectra with emission monitored at 730 nm were performed to assess whether the absorbed energy was transferred to chlorophyll *a*. As an estimate of photosynthetically active absorption, we normalized fluorescence excitation spectra to a^*_{ph} (676) (Sosik and Mitchell 1995; Moisan and Mitchell 1999). An example of total a_{ph} (λ) and photosynthetically active absorption, a^*_{ps} (λ) for a high light culture is shown in Fig. 4A. In each treatment, we observed chlorophyll *a* fluorescence in the UV absorption region which demonstrates that some of the absorbed UV excitation energy is transferred to chlorophyll *a*. Values of a^*_{ps} (330) were constant with light (Fig. 4B) while a^*_{ph} (330) increased by 7-fold (Fig. 1B). Values of ϕ_{fMAA} decreased with irradiance ranging from 5% to 18% of the total absorption for this spectral region (Fig. 4C). This ratio was proportional to the ratio of photosynthetic pigments to total pigments (Fig. 4D).

Relative fluorescence yields (ϕ_f) were calculated by dividing a_{ps} (λ) by a_{ph} (λ). Because we normalize each of our fluorescence excitation spectra to a_{ph} (676), ϕ_f (676) is equal to 1.0. We plot ϕ_f between 300 nm and 550 nm because the analytical noise of the two methods increases between 550 nm and 630 nm, due to weak absorption. In the UV region, ϕ_f values were low compared to those in the visible region (Fig. 5). They were ~20% of the red peak at the lower light intensities and were ~4% of the red peak at the photoinhibited light intensity (542 µmol quanta m^{-2} s^{-1}). Two peaks at 390 nm and 460 nm were observed which were 50% and 75% of the red peak, respectively. These ϕ_f peaks are located at chlorophyll *a* and chlorophyll *c* absorption maxima. From 350 to 495 nm, ϕ_f values for the highest light treatment were roughly half of the value found for the lower light intensities. DD + DT did not transfer energy efficiently to PSII as indicated by decreases in ϕ_f (495), similar to results of Johnsen et al. (1997). For all cultures, ϕ_f were highest above 500 nm. The low-light-

Table 2 Pigmentation in *Phaeocystis antarctica*. Fluorometric and HPLC chl *a* concentrations per cell. Accessory pigments are ratios to HPLC chl *a* (w:w). Chlorophyll (*Chl*), 19′hexanoyloxyfucoxanthin (*19′*hex), fucoxanthin (*fuco*), diadinoxanthin (*DD*), and diatoxanthin (*DT*). $n = 2$ samples for each irradiance

Light intensity µmol quanta m^{-2} s^{-1}	Pg per cell		Ratio to HPLC chl *a* (w:w)				
	Fluor chl *a*	HPLC chl *a*	Chl ($c_1 + c_2 + c_3$)	19′hex	fuco	β-carotene	DD + DT
14	0.39	0.37	0.42	0.61	0.01	0.0034	0.015
37	0.46	0.44	0.41	0.64	0.03	0.0026	0.016
84	0.41	0.49	0.31	0.27	0.01	0.0100	0.070
151	0.36	0.33	0.33	0.37	0.01	0.0114	0.099
259	0.36	0.37	0.38	0.39	0.01	0.0111	0.077
400	0.27	0.29	0.26	0.30	0.04	0.0158	0.120
542	0.19	0.15	0.20	0.23	0.01	0.0283	0.371

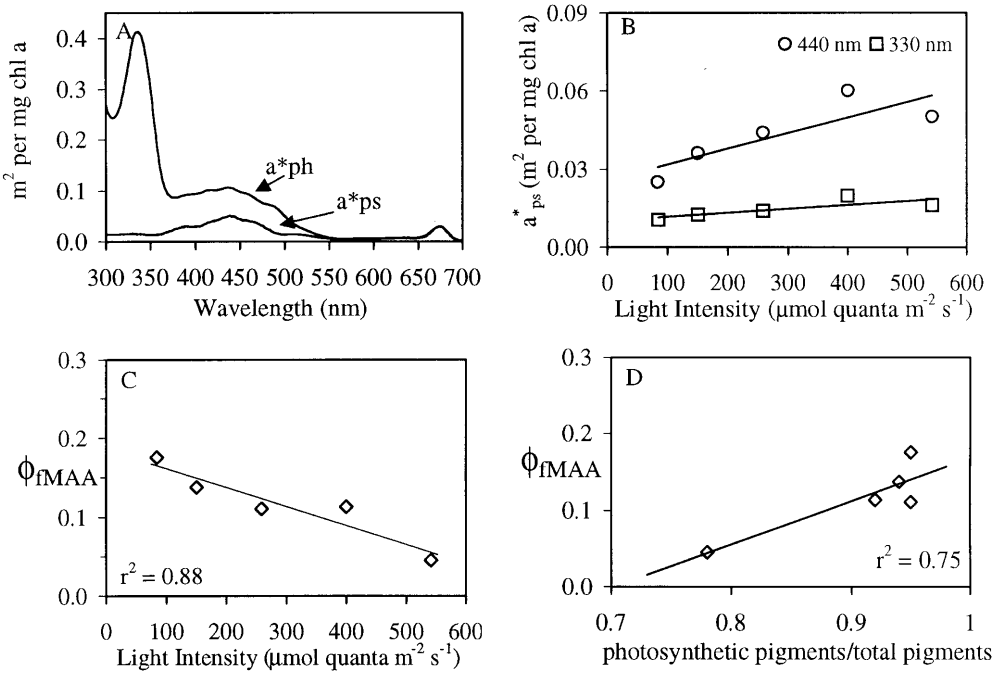

Fig. 4 **A** Spectra of a^*_{ph} (λ) and a^*_{ps} (λ) for *P. antarctica* grown at 542 µmol quanta m^{-2} s^{-1}. **B** Relationship between a^*_{ps} at 330 nm and 440 nm and light intensity. Regression not significant for relationship of a^*_{ps} with light (330;ANOVA, $P < 0.05$). **C** Relationship between ϕ_{fMAA} and irradiance. **D** Relationship between ϕ_{fMAA} and the fraction of photosynthetic pigments of total photosynthetic pigments. Regressions in **C** and **D** are significantly different from 0 (ANOVA, $P > 0.05$)

acclimated cultures had highest values; the lowest yield was observed for the photoinhibited treatment. Our observations from 400 to 500 nm are similar to results of Mitchell and Kiefer (1988a and b) for subtropical phytoplankton and cultures for Antarctic phytoplankton populations (Neori et al. 1984). Our results in the visible are similar to previous reports, but the very low values of a_{ps} in the MAA absorption band implies that the UV energy transferred to chlorophyll *a* fluorescence is absorbed by photosynthetic pigments and not MAAs.

Self-shading by MAAs

The efficiency factor for self-shading of a single cell (J_{tot}) at 330 nm was estimated using a_{ph} (330) (Fig. 6A) and radius (Fig. 6B) and ranged from 0.60 to 0.73. Both a^*_{ph} (330) and radius increased significantly at higher PAR irradiance (Fig. 6A, B). Figure 6C shows that J_{tot} (330) is lower than the absorption efficiency, Q_a (330) nm, calculated according to Morel and Bricaud (1981), with an increase at higher light intensities (Fig. 6D).

Using two different estimates for J_0, S factors were calculated to describe the efficiency of UV absorption (J_{tot}) compared to the efficiency of a cell with minimal UV absorption (J_0). When J_0 was calculated from *y*-intercept values of a_{ph} (330) and radius values versus PAR (Fig. 6A, B), S values ranged from 0.37 to 0.55 (Table 3). When J_0 was calculated from cellular radius values and a_{ps} (330), S ranged from 0.39 to 0.67 (Table 3). Because it is virtually impossible to determine the true J_0 for evaluating S, the good agreement between these two independent methods provides confidence in the overall magnitude, and range of variability, of our estimates of S due to MAA absorption.

Discussion

UV absorption due to mycosporine-like amino acids

The HPLC chromatograms indicated that mycosporine-glycine, shinorine, and mycosporine-glycine valine were responsible for the UV absorption in *Phaeocystis*

antarctica. Our results differ from those of Bidigare et al. (1996) who showed that a natural *Phaeocystis* population had only mycosporine-glycine valine. The MAAs in our *P. antarctica* cultures were among the MAAs described in mixed Antarctic populations including *Phaeocystis* (Dunlap et al. 1995). Our values of MAA content per cell are an order of magnitude below the values for diatoms given by Riegger and Robinson (1997), but our values are similar to theirs on a per-cell-volume basis.

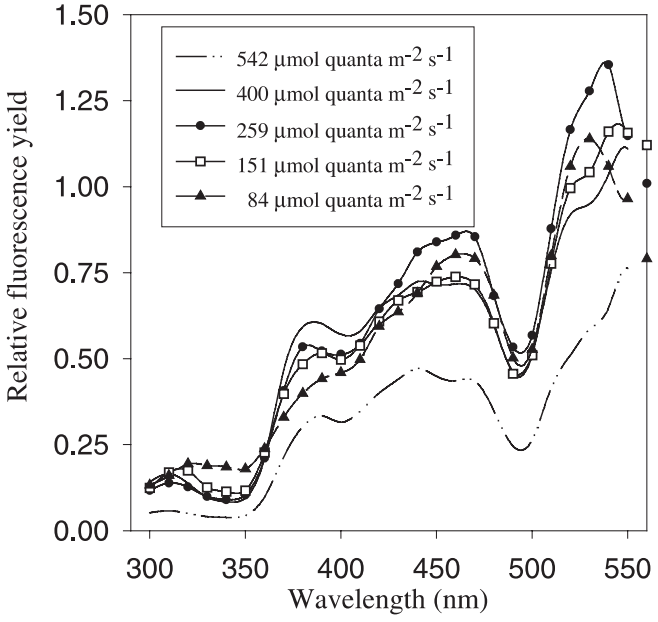

Fig. 5 Spectral dependence of chlorophyll *a* fluorescence yields for *P. antarctica* grown between 84 and 542 µmol quanta m^{-2} s^{-1}

Dependence of UV absorption on PAR intensity

We found significant changes in chlorophyll-specific UV absorption induced by PAR. UV absorption peaked between 330 nm and 336 nm. Spectral shifts in peak in vivo absorption are consistent with the maximal in vitro peaks and relative concentrations for the different MAAs (Fig. 2B). UV absorption peaked at 330 nm at the lowest light treatments when shinorine was the dominant MAA. At irradiances greater than 259 µmol quanta m^{-2} s^{-1}, UV absorption peaked at 336 nm (Fig. 1B), which is consistent with increases in the concentrations of shinorine and mycosporine-glycine valine relative to mycosporine glycine (Fig. 3).

Our ratios of a_{ph} (330) to a_{ph} (676) agree well with those of an Antarctic population that had characteristic prymnesiophyte pigmentation of *Phaeocystis pouchetii* (Vernet et al. 1994). Our a_{ph} (330:676) value at 85 µmol quanta m^{-2} s^{-1} is approximately half of the in vivo values of a *P. antarctica* culture grown at 100 µmol quanta m^{-2} s^{-1} at 0 °C (Riegger and Robinson 1997). Our ratios of in vivo absorption at the MAA peak at 330 nm to the red peak at 676 nm are at least half of the ratio of UV absorbance at 323 nm to the red peak of methanol:tetrahydrofuran extracted cultures of *Phaeocystis* observed by Davidson and Marchant (1994). We observed peak absorption for methanol extracts of total MAAs at 323 nm (data not shown) compared to in vivo

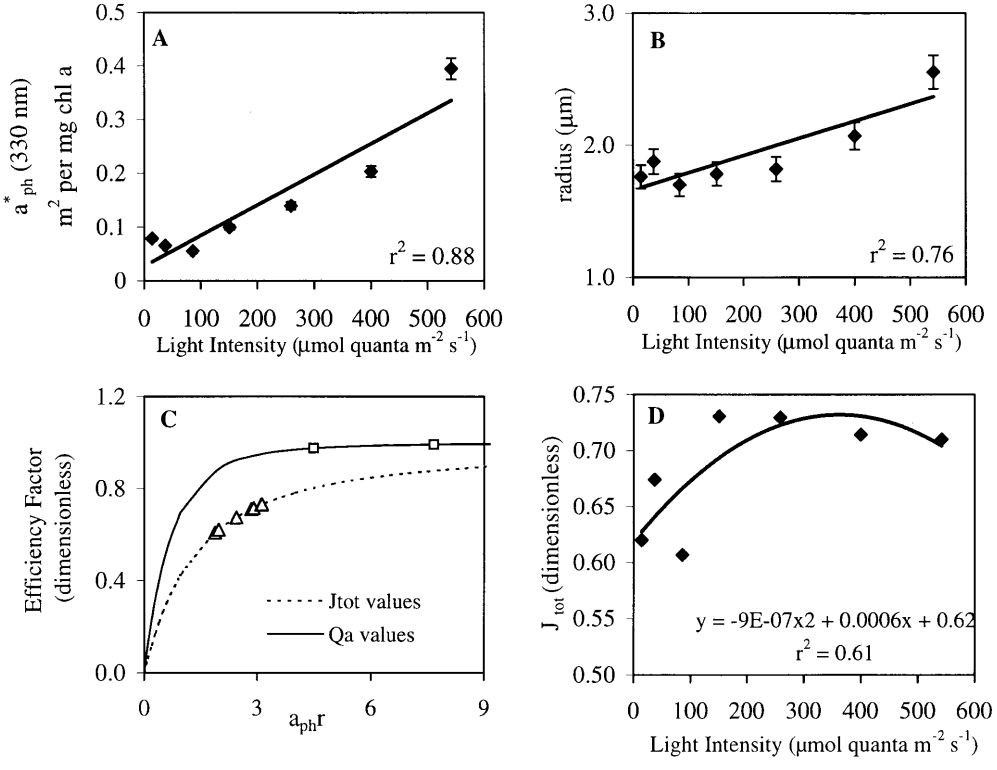

Fig. 6 The light-dependence of **A** a^*_{ph} (330). **B** Radius. **C** J_{tot} (*triangle*) and Q_a values (*square*) as a function of $a_{ph}r$. Model predictions using a_{ph} and r as input are indicated by *solid line* (Morel and Bricaud 1981) and the *dashed line* (Garcia-Pichel 1994). **D** J_{tot} values versus light intensity. Regressions in **A–C** are significantly different from 0 (ANOVA, $P > 0.05$)

Table 3 Cellular diameter, absorption, and sunscreen factors

Light intensity μmol quanta m^{-2} s^{-1}	Diameter (μm)	a^*_{ph} (330)	Sunscreen factor[a]	Sunscreen factor[b]
14	3.7	0.078	0.37	ND
37	3.5	0.065	0.46	ND
84	3.4	0.055	0.35	0.39
151	3.6	0.099	0.55	0.56
259	3.8	0.139	0.55	0.61
400	4.2	0.203	0.52	0.60
542	5.1	0.395	0.52	0.67

[a] J_0 was determined from the intercept at zero irradiance from regressions of a^*_{ph} and r
[b] J_0 is determined from a_{ps}

absorption peaks ≥330 nm. The high UV absorption relative to the red peak for the in vitro extract reported by Davidson and Marchant (1994) should be larger than our in vivo data, due to packaging effects. Absorption peaks in vitro often shift spectrally compared to in vivo absorption. A quantitative interpretation of MAA absorption requires determination of whole-cell absorption; absorption measured in organic extracts alone can only provide qualitative information, due to spectral shifts and uncertainty in package effects.

In an ecological context, the relationship between PAR and UV absorption is not surprising because they naturally co-vary. Therefore, increased PAR is a potential cue for increased UV radiation. It is to the advantage of phytoplankton to develop a common mechanism that responds to associated physical conditions that might limit or control growth. Interestingly, we found significant UV absorption at low light, as has been previously observed (Garcia-Pichel and Castenholz 1993; Vernet et al. 1994). The presence of significant UV absorption at low light may be advantageous to phytoplankton because it sets the lower limit for protection if phytoplankton are exposed to higher light intensities through mixing or changes in cloud cover, ice or ozone. The high baseline UV absorption combined with the ability to synthesize MAAs in hours (Carreto et al. 1990) and other methods of photoprotection (Lesser 1996; Mitchell and Karentz 1993) would be advantageous to a planktonic organism. Some MAAs may be excreted into the colonial mucilage and within the colony, which would afford *Phaeocystis* an even greater protection than if they are solely located within the cell. Vernet et al. (1998) showed that *Phaeocystis* is able to allocate its carbon reserves between the cell and the colonial mucilage.

MAA induction in *P. antarctica* appears to be regulated by PAR and UV radiation. In our study, MAA concentration, normalized on a per chlorophyll *a* or per carbon basis, increased as a pool with increasing PAR. The relationship between individual MAA induction under visible radiation has been characterized in coral (Gleason 1993), diatoms (Riegger and Robinson 1997), and dinoflagellates (Neale et al. 1998b). Individually, we found that the MAAs in *P. antarctica* responded differently to the intensity of PAR. Mycosporine-glycine valine and shinorine showed a response to light whereas mycosporine-glycine did not. Mycosporine-glycine may act as a precursor to the other MAAs present. Mycosporine-glycine does serve as a base for 17 known aminocyclohexenimines and 15 aminocyclohexenones, including the ones found in this study (Bandaranayake 1998).

The role of mycosporine-like amino acids as passive sunscreens

Researchers have hypothesize that absorbed UV radiation may be fluoresced at longer wavelengths and used for photosynthesis (Kawaguti 1969; Logan et al. 1990). To test whether the absorbed UV radiation is transferred to chlorophyll *a* for photosynthesis, we performed in vivo spectral fluorescence excitation on colonies of *P. antarctica*. Excitation spectra of chlorophyll *a* fluorescence, with emission monitored in the near infrared (730 nm), have been shown to be a good proxy for oxygen evolution action spectra (Neori et al. 1988). Fluorescence excitation spectra normalized to the red absorption peak have been used to estimate photosynthetically active absorption in phytoplankton (Sakshaug et al. 1991; Sosik and Mitchell 1995; Moisan and Mitchell 1999). The issue of scaling $F_{DCMU,}$ which originates from PSII, to estimate an absolute value of absorption by total photosynthetic pigments is subject to assumptions regarding relative absorption of PSI and PSII and energy transfer of absorbed photons to fluorescence. To estimate absorption of PSII, Johnsen et al. (1997) determined the fraction of chlorophyll *a* in PSI to total chlorophyll *a* and adjusted their F_{DCMU} in the red peak by this amount. Their scaled values of PSII absorption were 81–90% of total absorption at 676 nm. Our goal is to estimate total photosynthetically active absorption which includes absorption by both photosystems. Therefore, we normalize to total absorption in the red peak. Normalizing F_{DCMU} to total a_{ph} (676) may overestimate the true photosynthetic absorption in the blue-green region if the fluorescence excitation spectrum of PSII is augmented by antennae accessory pigments not present in PSI. The procedure of Johnsen et al. (1997) is valid for estimating absorption of PSII, but will slightly underestimate total photosynthetic absorption. Differences between these methods are small (10–20%).

In general, we found that, from 300 to 350 nm, a_{ps} was a small fraction (5–18%) of total absorption (Fig. 5). These low relative fluorescence yields suggest that a small fraction of UV-B energy is transferred to chlorophyll *a*. Chlorophyll *a* fluorescence from UV absorption apparently is not mediated by MAAs because it does not exhibit an emission peak where MAA absorption is maximal. We believe that the chlorophyll fluorescence from UV absorption originates from photosynthetic pigments. Values of ϕ_{fMAA} were positively correlated to the ratio of photosynthetic pigments to total HPLC pigments (Fig. 4D). Chlorophylls and fucoxanthins do absorb light between 300 and 350 nm in a

variety of solvents (Jeffrey et al. 1997); however, their true in vivo absorption characteristics are not well known. Oxygen evolution action spectra demonstrate photosynthetic activity in the UV region with shapes similar to our in vivo F_{DCMU} spectra (Neori et al. 1988). Based on low relative fluorescence yields in the UV region and previous evidence for photosynthetic pigment activity in the UV region, we conclude that energy absorbed by MAAs is not transferred to chlorophyll *a* and does not participate in photosynthesis. MAAs most likely act as a passive sunscreen, which is supported by the observation that MAAs are located in the cytoplasm (Garcia-Pichel and Castenholz 1993) and are not coupled to the photosystems. Because MAAs are not part of the photosynthetic antenna, there is no physical mechanism that would allow them to share excited electrons with the photosynthetic unit.

Increased MAA concentration per cell carbon with PAR implies biochemical accumulation or induction of MAA synthesis. We hypothesize that MAA induction is regulated by the flux absorbed by photosynthetic pigments that exceeds the capacity of cellular biochemistry to process the energy. For MAAs to be induced in this manner, feedback must occur from the photosynthetic apparatus to the biochemical pathway for genetic expression of enzymes that are required in MAA synthesis. This hypothesis accounts for the increases in MAAs due to PAR intensity, as we have shown. Clearly, light acclimation of MAA cellular concentrations are controlled by some mediator that varies in response to total cellular intercepted flux, and MAA induction may also be controlled by the same mediator. A mechanism such as this is plausible because UV radiation and photosynthetically available radiation naturally co-vary. Therefore, the proposed mechanism allows for an enhancement of UV absorption when cells are exposed to high light, even if UV-A or UV-B is negligible. However, MAA accumulation also may be due to disruption of a metabolic pathway (Goes et al. 1995), rather than induction. Certainly both processes could occur simultaneously.

Absorption efficiency and sunscreen factors

We calculated *S* factors based on the model of Garcia-Pichel (1994) in order to estimate the contribution of MAAs to the sunscreen effect. Our approach differs from experiments that compare UV to PAR treatments (e.g. Riegger and Robinson 1997). We use two different methods for calculating *S* factors, and they differ in how we estimated the variable, J_0 (330). Absorption at 330 nm is contributed mostly by MAAs and photosynthetic pigments. Absorption by RNA, DNA, amino acids, and proteins at 330 nm is minor (Stryer 1995). The estimation of J_0 is critical since treatments are compared to this value in order to estimate the sunscreen potential of MAAs. Therefore, the absorption of non-screening components, such as photosynthetic pigments, nucleic acids, and proteins, must be accounted for in the calculation of J_0. To estimate J_0 accurately, we attempt to estimate absorption contributed by cellular constituents other than MAAs. We found significant MAA concentrations, as other studies have shown, under conditions of low light or no UV radiation (Garcia-Pichel and Castenholz 1993; Vernet et al. 1994; Riegger and Robinson 1997). Estimates of *S* for MAAs will be underestimated if control cultures in experiments have significant MAA concentrations. To our knowledge, some UV absorption is always observed for phytoplankton, and therefore the contribution of photosynthetic pigments and other cellular components contributing to UV absorption should be taken into account when estimating J_0. Experiments where *S* for MAAs in different treatments only accounts for the differences in MAA absorption, but does not consider the contribution to *S* made by MAAs in the control culture.

Our estimates of J_0 based on the *y*-intercept values for regressions of a_{ph} and radius on PAR take into account the absorption by photosynthetic pigments, MAAs and proteins. When estimating *S* for MAAs, the J_0 derived with this method will be overestimated because MAAs are observed even at the lowest growth irradiance studied, and may always be present at low concentrations. Overestimates in J_0 will result in underestimates of *S*. The second method based on setting J_0 equal to a_{ps} (330) quantitatively accounts for the absorption by photosynthetic pigments and excludes absorption by MAAs, proteins, RNA, DNA or other cellular material. Therefore, using a_{ps} (330) to estimate J_0 will result in an underestimate because it accounts only for the absorption due to photosynthetic pigments. For each available treatment, our values of a_{ps} (330) were lower than when the *y*-intercept values for a_{ph} and radius with respect to PAR were used. Estimates of *S* for the two methods differ by 10–15% (Table 3), and we believe that the true value of *S* lies between our two estimates. The relatively high *S* factors suggest that MAAs make a significant contribution to UV screening, and that high visible radiation can induce MAA accumulation. The MAA pool appeared to be the dominant contributor to the variations in *S* (330), whereas changes in diameter contributed approximately 10% to the overall variation. Because previous investigators have found that UV absorption is enhanced under UV conditions compared to PAR conditions (Marchant et al. 1991), our *S* factors may not represent the full potential that MAAs provide to *P. antarctica* in nature.

Several cell characteristics other than MAAs may contribute to the efficiency of *P. antarctica* to enhance self-shading at high light. Individual cell diameter increased in response to increasing light. Our observations are consistent with results of Karentz et al. (1991) that decreased diatom surface area to volume ratios decreased the chances of UV cellular damage. Diatoms have also been observed to enlarge their cell volume spontaneously without dividing when exposed to UV radiation (Karentz et al. 1991). Because *P. antarctica* cells are embedded in a gelatinous matrix, light must be

transmitted through the colony and the fluid-filled space, which might enhance total UV attenuation if MAAs are excreted into the fluid-filled space or mucilage. Therefore, we expect that the self-shading factor for the entire colony will be underestimated because we use single-cell diameter in our calculations.

Conclusion

Significant variations in UV absorption in *Phaeocystis antarctica* are due to mycosporine-glycine, shinorine, and mycosporine-glycine valine. The total pool of MAAs and UV absorption increased with irradiance while photosynthetic pigments decreased. The combination of these factors resulted in large changes of UV absorption relative to cellular chlorophyll or carbon. Increases in MAA concentration and cell diameter at high light result in significant screening of UV flux by MAAs, which will protect photosynthetic pigments as well as other cell components. The low efficiency of chlorophyll fluorescence for UV absorption implies that MAAs do not transfer energy to chlorophyll *a* and therefore do not participate in photosynthesis. As light intensities increase during spring bloom initiation in Antarctica, UV-absorbing compounds may offer *Phaeocystis* spp. an advantage over other taxa that lack an ability to accumulate MAA compounds. More explicit experiments to evaluate the role of MAAs in photoprotection against UV radiation for various taxa and the mechanisms of induction of MAAs are still required to advance our understanding of their physiological and ecological roles.

Acknowledgements We thank S. Cheng for excellent technical assistance, K. Whitehead for her help in running MAA samples, method development, excellent advice and encouragement. M.P. Lesser and K. Walsh for conducting the secondary calibration, M. Vernet for insightful recommendations throughout this study and comments on earlier versions of the manuscript, M. Olaizola and R. Goericke for assistance with HPLC analysis and thoughtful discussions regarding photosynthetic pigment data, SIO Analytical Facility and staff (Bill Paplawsky and Kevin Walda) for technical support. We thank Brian Palenik and the reviewers for their comments which greatly improved the manuscript. Support for this work was provided by ONR grant N00014-98-1-0004 to B.G.M. and a NASA Earth System Science Fellowship NGT 5-30036 to T.A.M.

References

Arrigo KR (1994) Impact of ozone depletion on phytoplankton growth in the Southern Ocean: large-scale spatial and temporal variability. Mar Ecol-Progr Ser 114: 1–12

Bandaranayake WM (1998) Mycosporines: are they nature's sunscreens? Natural Product Reports: 159–172

Bidigare RR, Iriarte JL, Kang S-H, Karentz D, Ondrusek ME, Fryxell GA (1996) Phytoplankton: quantitative and qualitative assessments. In: Ross RM, Hofmann EE, Quetin LB (eds) Foundations for ecological research west of the Antarctic Peninsula, vol 70. American Geophysical Union, Washington, DC, pp 173–198

Bricaud A, Morel A, Prieur L (1983) Optical efficiency factors of some phytoplankters. Limnol Oceanogr 28: 816–832

Brody E, Mitchell BG, Holm-Hansen O, Vernet MV (1992) RACER 3: species-specific variations of the absorption coefficient in the Gerlache Strait. Antarct J US 27: 160–162

Caldwell MM, Camp LM, Warner CW, Flint SD (1986) Action spectra and their key role in assessing biological consequences of solar UV-B radiation change. In: Worrest RC, Caldwell MM (eds) Stratospheric ozone reduction. Solar ultraviolet radiation and plant life. Springer, New York, Berlin Heidelberg, pp 87–111

Carreto JI, Carignan MO, Daleo G, De Marco SG (1990) Occurrence of mycosporine-like amino acids in the red tide dinoflagellate *Alexandrium excavatum:* UV-photoprotective compounds? J Plankton Res 12: 909–921

Cullen JJ, Neale PJ, Lesser MP (1992) Biological weighting function for the inhibition of phytoplankton photosynthesis by ultraviolet radiation. Science 258: 646–650

Davidson AT, Marchant HJ (1994) The impact of ultraviolet radiation on *Phaeocystis* and selected species of Antarctic marine diatoms. Ultraviolet radiation and biological research in antarctica. In: Weiler CS, Penhale PA (eds) Antarctic Research Series 62. American Geophysical Union, Washington, DC, pp 187–205

Dunlap WC, Rae GA, Helbling EW, Villafañe VE, Holm-Hansen O (1995) Ultraviolet-absorbing compounds in natural assemblages of Antarctic phytoplankton. Antarct J US 30: 323–325

Dunlap WC, Chalker BE, Oliver JK (1986) Bathymetric adaptations of reef-building corals at Davies Reef, Great Barrier Réef, Australia. III. UV-B absorbing compounds. J Exp Mar Biol Ecol 104: 239–248

Dunlap WC, Yamamoto Y (1995) Small-molecule antioxidants in marine organisms: antioxidant activity of mycosporine-glycine. Comp Biochem Physiol 112B: 105–114

Garcia-Pichel F (1994) A model for internal self-shading in planktonic organisms and its implications for the usefulness of ultraviolet screens. Limnol Oceanogr 39: 1704–1717

Garcia-Pichel F, Castenholz RW (1993) Occurrence of UV-absorbing, mycosporine-like compounds among cyanobacterial isolates and an estimate of their screening capacity. Appl Environ Microbiol 59: 163–169

Gleason DF (1993) Differential effects of ultraviolet radiation on green and brown morphs of the Carribean coral *Porites asteroides*. Limnol Oceanogr 38: 1452–1463

Goes J, Handa N, Taguchi S, Hama T (1995) Changes in the patterns of biosynthesis and composition of amino acids in a marine phytoplankter exposed to ultra-violet-B radiation: nitrogen limitation implicated. J Photochem Photobiol 62: 703–710

Gomez E, Benjamin V, Figueroa F, Karsten U (1998) Effects of solar radiation on photosynthesis, UV-absorbing compounds and enzyme activities of the green alga *Dasycladus vermicularis* from southern Spain. J Photochem Photobiol 47: 46–57

Guillard RRL, Ryther JH (1962) Studies on marine planktonic diatoms. I. *Cyclotella nana* Hustedt and *Detonula confervacea* (Cleve) Gran. Can J Microbiol 8: 229–239

Helbling EW, Villafañe VE, Ferrario M, Holm-Hansen O (1992) Impact of natural ultraviolet radiation on rates of photosynthesis and on specific marine phytoplankton species. Mar Ecol Prog Ser 80: 89–100

Herrmann H, Hader D-P, Ghetti F (1997) Inhibition of photosynthesis by solar radiation in *Dunaliella salina*: relative efficiencies of UV-B, UV-A and PAR. Plant Cell Environ 20: 359–365

Holm-Hansen O, Lorenzen CJ, Holmes RW, Strickland JDH (1965) Fluorometric determination of chlorophyll. J Cons Explor Int Mer 30: 3–15

Holm-Hansen O, Mitchell BG, Vernet M (1989) Ultraviolet radiation in Antarctic waters: effect on rates of primary production. Antarct J US 24: 177–178

Jeffrey SW, Mantoura RFC, Bjørnland T (1997) Data for the identification of 47 key phytoplankton pigments. In: Jeffrey

SW, Mantoura RFC, Wright SW (eds) Phytoplankton pigments in oceanography. Monographs on oceanographic methodology. UNESCO, France, pp 661

Johnsen G, Nelson NB, Jovine RVM, Prezélin BB (1994) Chromoprotein- and pigment-dependent modeling of spectral light absorption of two dinoflagellates, *Prorocentrum minimum* and *Heterocapsa pygmaea*. Mar Ecol Prog Ser 114: 245–258

Johnsen G, Prezélin B, Jovine RVM (1997) Fluorescence excitation spectra and light utilization in two red tide dinoflagellates. Limnol Oceanogr 42: 1166–1177

Karentz D (1991) Ecological considerations of Antarctic ozone depletion. Antarctic Science 3: 3–11

Karentz D (1994) Ultraviolet tolerance mechanisms in Antarctic marine organisms. In: Weiler CS, Penhale PA (eds) Ultraviolet radiation in Antarctica: measurements and biological effects. American Geophysical Union: Ant Res Ser, pp 93–110

Karentz D, Spero HJ (1995) Response of a natural *Phaeocystis* population to ambient fluctuations of UVB radiation caused by Antarctic ozone depletion. J Plankton Res 17: 1771–1789

Karentz D, Cleaver JE, Mitchell DL (1991) Cell survival characteristics and molecular responses of Antarctic phytoplankton to ultraviolet-B radiation. J Phycol 27: 326–341

Kawagutti J (1969) Effect of the green fluorescent pigment on the productivity of the reef corals. Micronesia 5: 313

Kopf U, Heinz J (1984) 2,7-Bis(diethylamino)phenazoxonium chloride as a quantum counter for emission measurements between 240 and 700 nm. Anal Chem 56: 1931–1935

Lesser MP (1996) Acclimation of phytoplankton to UV-B radiation: oxidative stress and photoinhibition of photosynthesis are not prevented by UV-absorbing compounds in the dinoflagellate *Prorocentrum micans*. Mar Ecol Prog Ser 132: 287–297

Lesser MP, Cullen JJ, Neale PJ (1994) Carbon uptake in a marine diatom during acute exposure to ultraviolet B radiation: relative importance of damage and repair. J Phycol 30: 183–192

Lesser MP, Neale PJ, Cullen JJ (1996) Acclimation of Antarctic phytoplankton to ultraviolet radiation: ultraviolet-absorbing compounds and carbon fixation. Mol Mar Biol Biotech 5: 314–325

Logan A, Halcrow K, Tomascik T (1990) UV excitation-fluorescence in polyp tissue of certain scleractinian corals from Barbados and Bermuda. Bull Mar Sci 46: 807–813

Lubin D, Frederick J, Booth CR, Lucas T, Neuschuler D (1989) Measurements of enhanced springtime ultraviolet radiation at Palmer Station, Antarctica. Geophys Res Lett 16: 783–785

Marchant HJ, Davidson AT, Kelly GJ (1991) UV-B protecting compounds in the marine alga *Phaeocystis pouchetii* from Antarctica. Mar Biol 109: 391–395

Mitchell DL, Karentz D (1993) The induction and repair of DNA photodamage in the environment. In: Young AR, Björn LO, Moan J, Nultsch W (eds) Environmental UV photobiology. Plenum Press, New York, pp 345–377

Mitchell BG, Kiefer DA (1988a) Chlorophyll *a* specific-absorption and fluorescence excitation spectra for light-limited phytoplankton. Deep-Sea Res 35: 639–663

Mitchell BG, Kiefer DA (1988b) Variability in pigment specific particulate fluorescence and absorption spectra in the northeastern Pacific Ocean. Deep-Sea Res 35: 665–689

Mitchell BG, Vernet M, Holm-Hansen O (1989) Ultraviolet light attenuation in Antarctic waters in relation to particulate absorption and photosynthesis. Antarct J US 24: 179–180

Mobley C, Stramski D (1994) Influences of microbial particles on oceanic optics. Proc SPIE – Int Soc Opt Eng 2258: 184–193

Moisan TA, Mitchell BG (1999) Photophysiological adaptation of *Phaeocystis antarctica* Karsten under PAR light limitation. Limnol Oceanogr 44: 247–258

Moisan TA, Olaizola M, Mitchell BG (1998) Xanthophyll cycling in *Phaeocystis antarctica* Karsten: changes in cellular fluorescence. Mar Ecol Prog Ser 169: 113–121

Morel A, Bricaud A (1981) Theoretical results concerning light absorption in a discrete medium, and application to specific absorption of phytoplankton. Deep-Sea Res 11: 1375–1393

Neale PJ, Davis RF, Cullen JJ (1998a) Interactive effects on ozone depletion and vertical mixing on photosynthesis of Antarctic phytoplankton. Nature 392: 585–589

Neale PJ, Banaszak A, Jarriel CR (1998b) Ultraviolet sunscreens in *Gymnodinium sanguineum* (Dinophyceae): mycosporine-like amino acids protect against inhibition of photosynthesis. J Phycol 34: 928–938

Neori A, Holm-Hansen O, Mitchell BG, Kiefer DA (1984) Photoadaptation in marine phytoplankton. Plant Physiol 76: 518–524

Neori A, Vernet M, Holm-Hansen O, Haxo FT (1988) Excitation spectra of chlorophyll far-red fluorescence compared to chlorophyll red fluorescence and to photosystem II photosynthetic action spectra in algae. Mar Ecol Prog Ser 44: 297–302

Peterson PJM, Smith RC, Patterson KW (1995) A biological weighting function for phytoplankton growth inhibition. In: Gulko D, Jokiel PL (eds) Ultraviolet radiation and coral reefs. HIMB Tech, pp 51–60

Quesada A, Mouget J-L, Vincent WF (1995) Growth of Antarctic cyanobacteria under ultraviolet radiation: UVA counteracts UVB inhibition. J Phycol 31: 242–248

Riegger L, Robinson D (1997) Photoinduction of UV-absorbing compounds in Antarctic diatoms and *Phaeocystis antarctica*. Mar Ecol Prog Ser 160: 13–25

Sakshaug E, Johnsen G, Andresen K, Vernet M (1991) Modeling of light-dependent algal photosynthesis and growth: experiments with the Barents Sea diatoms *Thalassiosira nordenskioeldii* and *Chaetoceros furcellatus*. Deep-Sea Res 38: 415–430

Schick JM, Lesser MP, Stochaj WR (1991) Ultraviolet radiation and photooxidative stress in zooxanthellae Anthozoa: the sea anemone *Phyllodiscus semoni* and the octocoral *Clavularia* sp. Symbiosis 10: 145–173

Schofield O, Kroon BMA, Prezélin BB (1995) Impact of ultraviolet-B radiation on photosystem II activity and its relationship to the inhibition of carbon fixation rates for Antarctic ice algae communities. J Phycol 31: 703–715

Smith RC, Cullen JJ (1995) Effects of UV radiation on phytoplankton. US National Report to International Union of Geodesy and Geophysics 1991–1994. Rev Geophys Suppl: 1211–1223

Smith RC, Prézelin BB, Baker KS, Bidigare RR, Boucher NP, Coley T, Karentz D, MacIntyre S, Matlick HA, Menzies D, Ondrusek ME, Wan Z, Waters KJ (1992) Ozone depletion: ultraviolet radiation and phytoplankton biology in Antarctic waters. Science 255: 952–959

Smith WO, Nelson DM (1986) The importance of ice-edge blooms in the Southern Ocean. BioScience 36: 251–257

Sosik HM, Mitchell BG (1995) Absorption by phytoplankton, photosynthetic pigments, and detritus in the California Current System. Deep-Sea Res 42: 1717–1748

Stryer L (1995) Biochemistry. Freeman, New York

Vernet M, Whitehead K (1996) Release of ultraviolet-absorbing compounds by the red-tide dinoflagellate *Gonyaulax polyedra*. Mar Biol 127: 35–44

Vernet M, Brody EA, Holm-Hansen O, Mitchell BG (1994) The response of Antarctic phytoplankton to ultraviolet light: absorption, photosynthesis, and taxonomic composition. Antarct Res Ser 62: 143–158

Vernet M, Matrai PA, Andreassen I (1998) Synthesis of particulate and extracellular carbon by phytoplankton in the Barents Sea. J Geophys Res Oceans V103(NC1): 1023–1037

Villafañe VE, Helbling EW, Holm-Hansen O, Chalker BE (1995) Acclimatization of Antarctic natural phytoplankton assemblages when exposed to solar ultraviolet radiation. J Plankton Res 17: 2295–2306

Whitehead KW (1996) Release of UV-absorbing compounds by marine phytoplankton and their effect on the absorption properties of particulate and dissolved organic matter. MS thesis, University of California, pp 98

Wright SW, Jeffrey SW, Mantoura RFC, Llewellyn CA, Bjørnland T, Repeta D, Welschmeyer N (1991) Improved HPLC method for the analysis of chlorophylls and carotenoids from marine phytoplankton. Mar Ecol Prog Ser 77: 183–196